Nonswelling, Ultralow Content Inverse Electron-Demand Diels–Alder Hyaluronan Hydrogels with Tunable Gelation Time: Synthesis and In Vitro Evaluation

Vianney Delplace, Philip E. B. Nickerson, Arturo Ortin-Martinez, Alexander E. G. Baker, Valerie A. Wallace, and Molly S. Shoichet*

Hyaluronan (HA) is a major component of the extracellular matrix and is particularly attractive for cell-based assays; yet, common crosslinking strategies of HA hydrogels are not fully tunable and bioorthogonal, and result in gels subject to swelling, which affects their physicochemical properties. To overcome these limitations, HA hydrogels based on the inverse electron-demand Diels–Alder (IEDDA) "click" reaction are designed. By crosslinking two modified HA components together, as opposed to using telechelic components, tunable gelation times as fast as 4.4 ± 0.4 min and as slow as 46.2 ± 1.8 min are achieved for facile use. By optimizing HA molar mass, ultralow polymer content hydrogels of 0.5% (w/v), resulting in minimal (<3–5% mass variation) to nonswelling (<1%), transparent and biodegradable hydrogels are synthesized. To demonstrate their versatility, the newly designed hydrogels are tested as matrices for 3D cell culture and retinal explant imaging where transparency is important. IEDDA hydrogels are cytocompatible with primary photoreceptors and enable multiphoton imaging of embedded retinal explants for double the time (>38 h) than agarose thermogels (<20 h). IEDDA HA hydrogels constitute a new hydrogel platform. They have low polymer content, tunable gelation time, and are stable, thereby making them suitable for a diversity of applications.

1. Introduction

Hyaluronan is a particularly compelling natural biomaterial;[1–8] yet, the bio-orthogonal crosslinking of HA hydrogels is challenging. Some systems require external stimuli (e.g., photochemistry) or catalysts/activating agents to crosslink, thereby providing a complex hydrogel system. Others use crosslinking chemistry that is unstable under physiological conditions (e.g., hydrazone, disulfide, Michael addition), resulting in uncontrolled degradation, while others either gel too slowly for effective cell encapsulation or are reversibly crosslinked (e.g., Diels–Alder),[9–11] thereby being inherently limited. Moreover, most hydrogels swell during formation and degradation,[12–15] which can be deleterious when injected into tissues and/or confined spaces. With the goal of synthesizing a minimally swelling HA hydrogel with low polymer content and tunable gelation, we optimized HA molar mass and used the inverse electron-demand Diels–Alder (IEDDA) "click" reaction as a crosslinking mechanism.

IEDDA reactions are bioorthogonal, compatible with physiological conditions, and have been studied in chemical biology;[16,17] however, only a handful of papers have reported their use for hydrogel design. For example, tetrazine–norbornene IEDDA-crosslinking has been demonstrated with hydrogels composed of gelatin,[18,19] alginate, polyethylene glycol (PEG), and hyaluronan.[20–24] Unfortunately, tetrazine degrades rapidly under physiological conditions[25] and all of these systems require high polymer content (typically 2–10%, w/v) for gelation, which impacts pipettability, swelling, and stiffness. While IEDDA is compelling

Dr. V. Delplace, Dr. A. E. G. Baker, Prof. M. S. Shoichet
Chemical Engineering and Applied Chemistry
University of Toronto
200 College Street, Toronto, ON M5S 3E5, Canada
E-mail: molly.shoichet@utoronto.ca
Dr. P. E. B. Nickerson, Dr. A. Ortin-Martinez, Prof. V. A. Wallace
Donald K. Johnson Eye Institute
Krembil Research Institute
University Health Network
Toronto, ON M5T 2S8, Canada

Dr. P. E. B. Nickerson
Department of Psychology
Nipissing University
100 College Dr. North Bay, Toronto, ON P1B8L7, Canada
Dr. A. E. G. Baker, Prof. M. S. Shoichet
Institute of Biomaterials and Biomedical Engineering
University of Toronto
164 College St., Toronto, ON M5S 3G9, Canada
Prof. V. A. Wallace
Department of Laboratory Medicine and Pathobiology
University of Toronto
27 King's College Circle, Toronto, ON M5S 1A1, Canada
Prof. V. A. Wallace
Department of Ophthalmology and Vision Sciences
University of Toronto
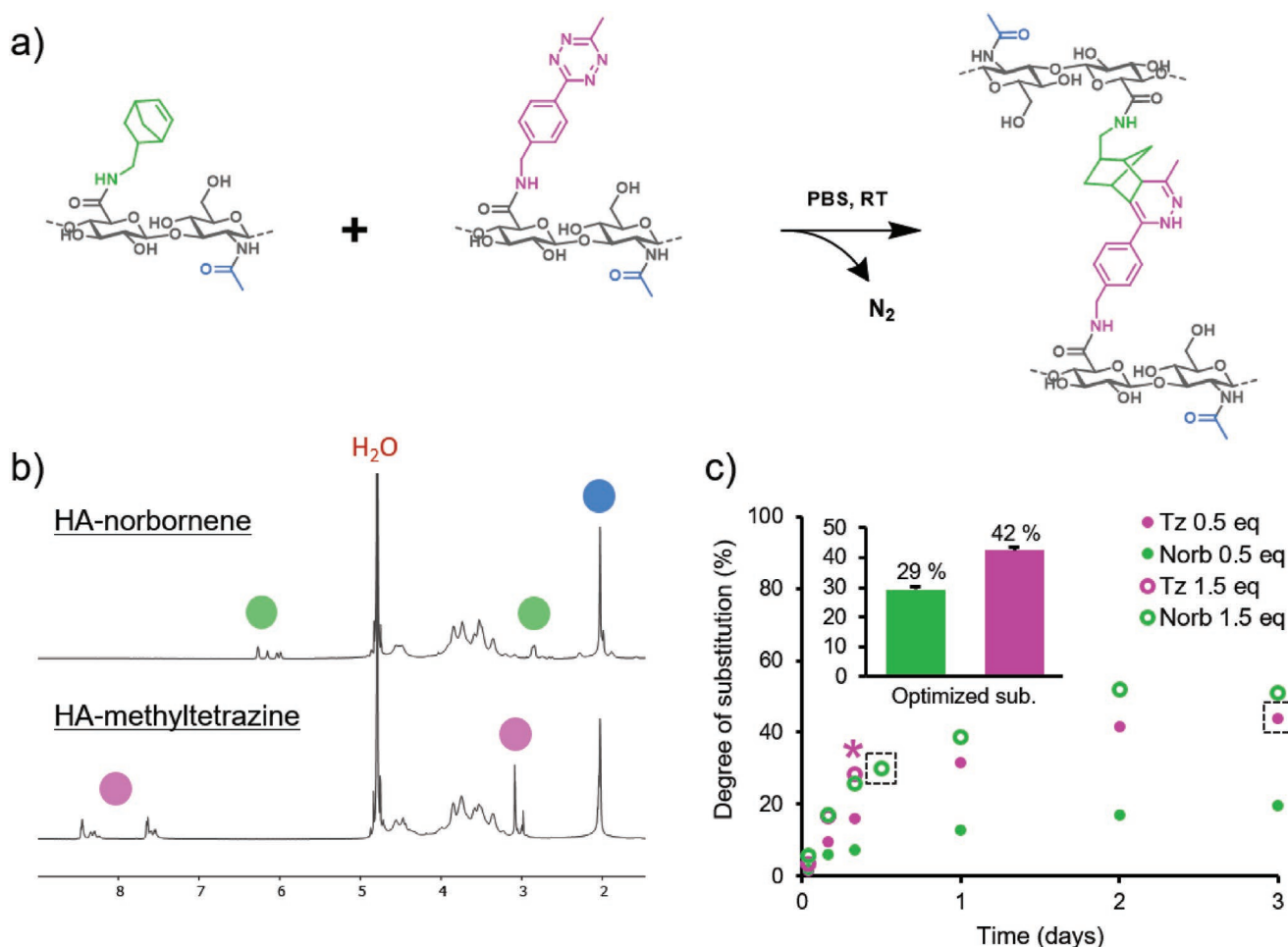340 College Street, Toronto, ON M5T 3A9, Canada

Figure 1. Inverse electron-demand Diels–Alder (IEDDA) HA–HA hydrogel. a) Schematic of IEDDA HA–HA hydrogel, where norbornene-modified HA reacts with methylphenyltetrazine-modified HA to form a stable hydrogel, at physiological pH (in PBS) and room temperature. The *N*-acetyl, norbornene, and methylphenyltetrazine chemical groups are highlighted in blue, green, and pink, respectively. b) Typical ^{1}H NMR (500 MHz, D$_2$O, δ) of HA–norbornene and HA–methylphenyltetrazine show successful substitution. The *N*-acetyl group of HA (3H at 2 ppm; blue circle) is used as a reference to calculate the degrees of substitution of norbornene (2H (CH=CH) at 5.8–6.2 ppm and 2H (CH$_2$–N) at 2.8 ppm; green circles) and methylphenyltetrazine (4H (phenyl) at 7.5–8.5 ppm and 3H (CH3) at 3.1 ppm; pink circles). In these examples, when normalized to the *N*-acetyl group of HA (3 H at 2 ppm), HA–norbornene showed a peak area at 5.8–6.2 ppm of 0.58, and HA–methylphenyltetrazine showed a peak area at 7.5–8.5 ppm of 1.68. These integrals correspond to substitutions of 29% and 42%, for HA–norbornene and HA–methylphenyltetrazine, respectively. c) Substitution kinetics of HA, using 0.5 eq (closed circles) or 0.75 eq (open circles) of norbornene (green) or methylphenyltetrazine (pink). * indicates the last time point before the precipitation of HA–methylphenyltetrazine when using 1.5 eq methylphenyltetrazine. The dashed squares indicate the optimal conditions of norbornene (1.5 eq; 12 h) and methylphenyltetrazine (0.5 eq; 3 days) substitution. As shown in the inner graph, these conditions showed good batch-to-batch reproducibility ($n = 3$; mean ± SD).

with tetrazine–norbornene, nitrogen bubbles, and pink-colored materials are typically produced, affecting their utility.

To optimize the IEDDA reaction, we replaced tetrazine with the more stable methylphenyltetrazine, thereby eliminating reagent degradation (**Figure 1**a). We crosslinked high and low molar mass HA at varying ratios, thereby achieving controlled gelation and minimal swelling. With this strategy, HA gels were produced with very low polymer content, optical transparency, and minimal nitrogen gas production. To demonstrate the utility of HA–HA crosslinking, these new IEDDA HA–HA hydrogels were compared to IEDDA HA–PEG hydrogels in terms of gelation time, stiffness, and swelling.

To gain greater insight into the biological utility of these IEDDA HA–HA hydrogels, we investigated them in the context of the retina because HA itself is a major component of the vitreous[26] and the retina ECM,[27–29] and is known to interact with cells via specific receptors, such as CD44 and RHAMM.[28,30] HA has been shown to promote the survival of primary mouse and retinal stem cell-derived rod photoreceptors both in vitro and in vivo through mTOR- and CD44-mediated pathways.[31,32] Moreover, the utility of HA as a scaffold component has been investigated in the context of retinal pigment epithelial (RPE) and retinal progenitor cell delivery, and adult retinal tissue culture.[33–35] Using cone-like photoreceptor cells,[36,37] we demonstrated that our newly designed IEDDA-crosslinked HA hydrogels are cytocompatible and allow cell encapsulation. We took advantage of the transparent, controlled gelation material for retinal explant

**ADVANCED
SCIENCE NEWS**

www.advancedsciencenews.com

**ADVANCED
FUNCTIONAL
MATERIALS**

www.afm-journal.de

immobilization and multiphoton imaging, showing great improvement in both image acquisition quality and preservation of the fluorescence reporter signal compared to the current standard agarose gels.[38]

2. Results and Discussion

2.1. Single-Step Synthesis of IEDDA Hydrogel Components: HA–Norbornene and HA–Methylphenyltetrazine

In this study, we replaced the commonly used phenyltetrazine with methylphenyltetrazine (Figure 1a). Electron-donating groups (e.g., alkyl) on tetrazines ensure hydrolytic stability at the expense of reactivity; thus, while ≈15 times less reactive than phenyltetrazine, methylphenyltetrazine was reported to be the most stable, yet still reactive, of the tetrazine derivatives in fetal bovine serum (FBS) at 37 °C.[25,39] It should be noted that strikingly different results have been reported on the stability of phenyltetrazine in PBS (≈75% after 12 h)[40] versus aminated phenyltetrazine in FBS (≈40% after 10 h).[25] The observed difference may result, in part, from interactions with serum proteins, and requires careful consideration of the effect of chemical modification on reagent stability. More importantly, methylphenyltetrazine derivatives showed high stability (≈80–95%) in both studies, further supporting our design rationale to use methylphenyltetrazine. The use of methylphenyltetrazine eliminates reagent degradation during component synthesis and hydrogel formation. HA was first modified with either 5-norbornene-2-methylamine or methylphenyltetrazine-amine (HCl salt), resulting in HA–norbornene or HA–methylphenyltetrazine, respectively, as characterized by ^{1}H NMR (Figure 1b). To optimize the substitution reactions, the kinetics of both HA–norbornene (240 kDa) and HA–methylphenyltetrazine (240 kDa) were investigated by ^{1}H NMR. At 0.5 eq of functional group (relative to HA carboxylic acid) and under similar reaction conditions (i.e., concentration, volume, time, temperature), the methylphenyltetrazine reaction reached a higher degree of substitution of 44% versus that with norbornene of 20% after 3 d, which may be due to steric effects and a difference in reactivity between the endo-exo norbornene isomers (Figure 1c). At higher equivalents (1.5 eq) of each functional group, methylphenyltetrazine-substituted HA precipitated, rendering it unusable, whereas norbornene substitution plateaued at 52%. HA–norbornene and HA–methylphenyltetrazine substitutions showed good batch-to-batch reproducibility (Figure 1c), and were fixed, for further investigation, to 29% ± 1% and 42% ± 2%, respectively. Both HA–norbornene and HA–methylphenyltetrazine could be easily dissolved in aqueous media (e.g., PBS or cell culture medium), and conveniently stored at 4 °C.

We synthesized HA–methylphenyltetrazine of different molar masses (i.e., 10, 20, 40, or 240 kDa), with a fixed substitution of ≈40% (Figure S1, Supporting Information), to investigate the effect of methylphenyltetrazine crosslinker molar mass on gelation with HA–norbornene (240 kDa). Since PEG is a common crosslinker, we synthesized 4-arm PEG–methylphenyltetrazine (5 kDa) and compared its gelation to HA–norbornene with that of HA–methylphenyltetrazine.

2.2. Physicochemical Properties of IEDDA HA–HA Hydrogels: Transparency, Swelling, and Rate of Gelation

To synthesize IEDDA HA hydrogels, HA–norbornene and HA–methylphenyltetrazine were reacted together. Since unreacted tetrazine derivatives are pink and reacted ones are colorless, we minimized the methylphenyltetrazine content such that the methylphenyltetrazine to norbornene molar ratio (mpT/N) is less than 1, ensuring colorless gels upon complete reaction. We designed hydrogels with low crosslink density to limit nitrogen formation; low polymer content to minimize pregel solution viscosity; low norbornene substitution to maximize HA bioactivity and biodegradability; and maximal methylphenyltetrazine substitution to reduce the amount of crosslinker for a given mpT/N ratio.

2.3. IEDDA HA–HA Hydrogels Are Transparent and Clear of Bubbles

We optimized the physicochemical properties of IEDDA HA–HA hydrogels in terms of be transparent, minimally swelling, and to have controlled gelation. Gels form rapidly, within 10 min upon mixing HA–norbornene and HA–methylphenyltetrazine (**Figure 2**a). While pregel solutions were pink due to the presence of methylphenyltetrazine, the color disappeared within hours, resulting in clear HA hydrogels. To quantify transparency, the refractive index of a typical IEDDA HA–HA hydrogel in PBS was first measured: 0.75% (w/v) HA–norbornene, 240 kDa HA–norbornene/240 kDa HA–methylphenyltetrazine, (i.e., 240/240), mpT/N = 0.25. A refractive index of 1.335 was observed both before and after gelation, which is similar to that of PBS, which has a refractive index of 1.333, demonstrating minimal effect of gelation.

As the tetrazine-norbornene reaction produces nitrogen (N$_2$), gas bubbles could form during gelation. In water at 37 °C, the saturation concentration of N$_2$ is ≈15 mg L^{-1}.[41] In 0.5–0.75% (w/v) IEDDA HA gels, the maximum concentration of N$_2$ produced is 22.6–35.3 mg L^{-1}, suggesting the possible formation of N$_2$ bubbles. To assess N$_2$ bubble formation in IEDDA HA gels, a qualitative macroscopic evaluation was performed using a scale of 1 to 4, with 1 indicating no visible bubbles and 4 indicating too many bubbles to count that are average to big. In the optimized IEDDA HA–HA hydrogels with low polymer content (up to 0.75% (w/v) HA–norbornene at mpT/N = 0.25), no visible bubbles were observed, independent of the molecular weight (MW) of HA (Figure S2, Supporting Information). Higher polymer content (i.e., crosslink density) led to the formation of nitrogen bubbles, of which number and size increased concomitantly with polymer content. The absence of bubbles in the optimized gels must result from gas exchange at the air–water interface, emphasizing the importance of the gel geometry. This is the first IEDDA system that is reproducibly clear of bubbles.[18,20–22] These results also highlight the importance of low crosslinking in IEDDA systems.

A transmittance study demonstrated the complete disappearance of the methylphenyltetrazine peak (typically at λ = 520 nm)[25,42] within 8 h at room temperature, and confirmed high transparency (transmittance >90%) of the material
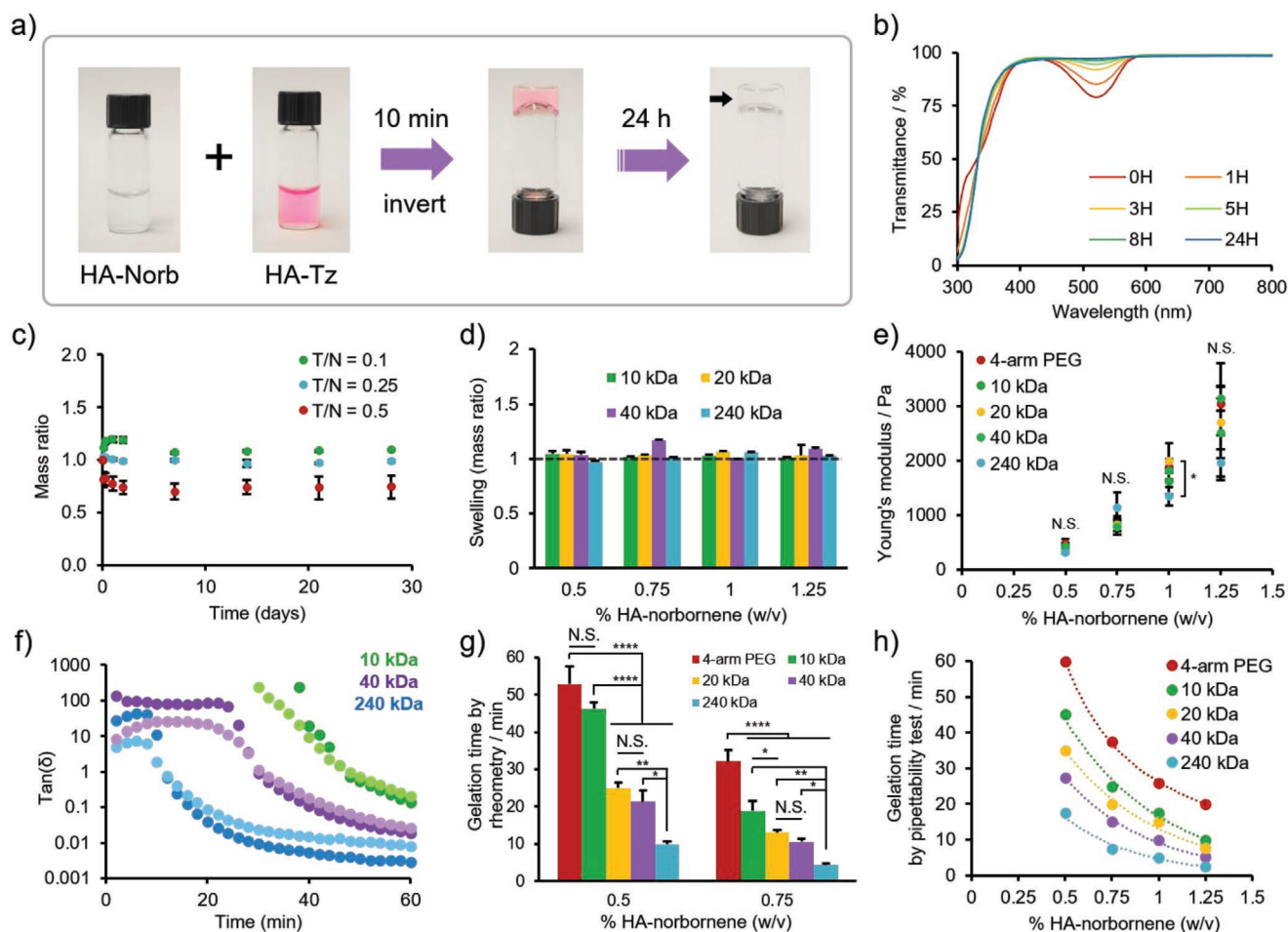
Figure 2. Inverse electron-demand Diels–Alder (IEDDA) HA–HA hydrogels rapidly form under physiological conditions and are tunable, transparent, nonswelling, and stable. a) Typical example of IEDDA HA–HA hydrogel (0.75% (w/v) HA–norbornene, 240/240 kDa; mpT/N = 0.25), where HA–norbornene and HA–methylphenyltetrazine are each easily dissolved in PBS, prior to mixing in a 1:1 volume ratio, and rapidly gel. Upon gelation, the pink color of methylphenyltetrazine disappears to form a clear hydrogel within 24 h. b) Transmittance over time of a 0.75% (w/v) HA–norbornene, 240/240 kDa HA–HA hydrogel (mpT/N = 0.25), measured at room temperature, confirming the transparency of the IEDDA HA–HA gels (transmittance ≥95%) and the rapid disappearance of the pink color of methyltetrazine (within 8 h). c) Swelling/stability study of 0.75% (w/v) HA–HA hydrogels at three different mpT/N molar ratios (i.e., 0.1, 0.25, and 0.5). The optimal ratio of 0.25 produces nonswelling HA–HA hydrogels, while hydrogels at a lower mpT/N ratio swell and hydrogels at higher mpT/N ratio contract. The data also show stabilization within 2 d, followed by long-term stability (at least one month) of the hydrogel at any mpT/N ratio. d) The nonswelling property of IEDDA HA–HA hydrogels, at a fixed mpT/N ratio of 0.25, is independent of both the molar mass of HA–methyltetrazine crosslinker (10, 20, 40, 240 kDa) and the HA–norbornene concentration (0.5% to 1.25% (w/v)). The dashed line indicates a mass ratio of 1, as guide for the eye for ideal nonswelling. e) The Young's modulus of IEDDA HA hydrogels, at a fixed mpT/N = 0.25, is independent of the nature of the crosslinker (HA vs PEG), the molar mass of HA–methyltetrazine crosslinker (10, 20, 40, and 240 kDa) and the HA–norbornene concentration (0.5% to 1.25% w/v). f) Loss tangent (tan(δ)) of 0.5% (w/v) IEDDA HA–HA hydrogels crosslinked with 10, 40, and 240 kDa HA–methyltetrazine with mpT/N = 0.25 and studied at two frequencies: 0.1 Hz (light dots) and 0.2 Hz (dark dots). The data highlight that the gelation time can be tuned by varying the molar mass of HA–methyltetrazine crosslinker. g) Average gelation time of various IEDDA HA–HA hydrogel formulations for two different HA–norbornene concentrations (0.5% and 0.75% (w/v)), comparing 4-arm PEG–methyltetrazine (5 kDa) and different HA–methyltetrazine crosslinkers (10, 40, and 240 kDa) at a fixed mpT/N = 0.25. The gelation time is defined as the intersection of two loss tangent curves from measurements at two frequencies: 0.1 and 0.2 Hz (n = 3; mean ± SD). h) Gelation time, measured by pipettability, of various IEDDA HA hydrogel formulations, as a function of HA–norbornene concentrations and comparing 4-arm PEG–methyltetrazine (5 kDa) and different HA–methyltetrazine (10, 40, and 240 kDa) crosslinkers, at a fixed mpT/N = 0.25. Statistical significance was determined using one-way ANOVA with Tukey's posthoc test: N.S. = not significant, $*p < 0.05$, $**p < 0.01$, $***p < 0.001$.

over the entire visible light spectrum (Figure 2b). High transparency was maintained at a mpT/N ratio of 0.5 as well. Faster methylphenyltetrazine conversion was observed at 37 °C compared to room temperature (transmittance >90% within 3 h vs 8 h), reflecting the faster gelation at increased temperature (Figure S3, Supporting Information).

2.4. IEDDA HA–HA Hydrogels Are Nonswelling, Stable, and Soft

Stability and swelling are key parameters for hydrogels[43–46] and thus the swelling properties of IEDDA HA–HA hydrogels were investigated. The concentration of HA–norbornene was fixed to

**ADVANCED
SCIENCE NEWS**
www.advancedsciencenews.com

**ADVANCED
FUNCTIONAL
MATERIALS**
www.afm-journal.de

0.75% (w/v), and various mpT/N molar ratios (0.1, 0.25, and 0.5) were tested (Figure 2c). Measuring hydrogel mass over time, we observed that a low mpT/N ratio of 0.1 led to hydrogel swelling whereas a high mpT/N ratio of 0.5 led to hydrogel shrinking. Hydrogels at a high mpT/N ratio also shrunk in the presence of a large excess of unreacted tetrazine quencher (i.e., free norbornene), suggesting that the contraction observed did not result from hydrophobic interactions between unreacted tetrazines or further crosslinking upon water addition (Figure S4, Supporting Information). We therefore attributed shrinking at the higher mpT/N ratio solely to the distance between crosslinks, as previously suggested by others.[44] Remarkably, we found that the optimal mpT/N ratio of 0.25 led to nonswelling HA hydrogels (<3% variation in mass) and that these hydrogels are stable over weeks. Using the same mpT/N ratio of 0.25, similar minimal-to-nonswelling hydrogels were produced over a range of HA–norbornene concentrations (0.5%, 0.75%, 1.0%, and 1.25% (w/v)) and with various HA–methylphenyltetrazine crosslinkers (of 10, 20, 40, and 240 kDa) (Figure 2d). These data suggest that the minimal swelling of IEDDA HA gels is independent of both HA concentration and molar mass (within the range tested), and mainly depends on the effective molecular weight between crosslinks.[44] Strategies to design nonswelling hydrogels typically add hydrophobic polymers, which counteract swelling by shrinking (e.g., PNIPAAM).[43,44,47–49] Most of these studies were performed on PEG gels, and degraded within 5 to 15 days due to hydrolyzable crosslinking methods[48,49] or shrunk before showing long-term stability.[44,50] While long-term stability of HA gels was demonstrated in the past,[51] this is the first report of nonswelling, chemically crosslinked HA hydrogels. As PEG crosslinkers did not allow the synthesis of nonswelling IEDDA gels (Figure S5, Supporting Information), we only pursued with the more tunable, multifunctional HA crosslinkers for the remainder of our studies.

The Young's moduli of IEDDA HA–HA hydrogels were compared as a function of HA–norbornene content for each of HA–methylphenyltetrazine crosslinkers at 10, 20, 40, and 240 kDa (Figure 2e). Interestingly, at low HA–norbornene concentrations (0.5% and 0.75% (w/v)), the final stiffness was independent of the nature (PEG vs HA) and molar mass of the crosslinker. However, at higher polymer content (typically 1.25% (w/v)), the Young's modulus increased inversely with the HA crosslinker molar mass, reflecting the impact of the limited diffusion of high MW chains during network formation.[52] While the synthesis of stiff IEDDA HA hydrogels is limited by HA viscosity and nitrogen bubbles, hydrogels with stiffnesses between 500 and 1500 Pa could be easily synthesized, making this system ideal for soft material applications.

2.5. IEDDA HA–HA Hydrogels Form within Minutes

Having tunable gelation times enables hydrogels to be adapted to accommodate a breadth of applications. The gelation time of IEDDA HA–HA hydrogels was investigated using dynamic shear rheometry and pipettability. We evaluated the gelation time of IEDDA HA hydrogels by rheometry, characterizing the intersection of loss tangent, tan(δ), curves measured at various frequencies.[53] At constant HA concentration and fixed norbornene and methylphenyltetrazine substitutions, increasing the molar mass of the HA–methylphenyltetrazine crosslinker resulted in decreased gelation time (Figure 2f). For example, increasing the molar mass of the HA–methylphenyltetrazine crosslinker from 10 to 240 kDa decreased the gelation time of a 0.5% (w/v) HA–norbornene (240 kDa) gel from 46 to 12 min. The reduced time to gelation with greater molar mass reflects both increased polymer entanglement[54] and more reactive functional sites per polymer chain; thus, the probability of having multiple reactions on a polymer chain increases for a given reaction rate as stated by the Flory–Stockmayer Theory.[55,56] In this way, gelation time can be tailored from minutes to hours by simply adjusting the molar mass of the HA crosslinker. Moreover, as we showed that final stiffness is independent of HA–methylphenyltetrazine molar mass, gelation time can be tuned independently of stiffness, which is a unique feature. As expected, increasing the HA–norbornene concentration at a constant mpT/N ratio also decreased gelation time, allowing us to tune both polymer content and HA molar mass to achieve the desired gelation time (Figure 2g).

Commercially available, PEG is often used as a crosslinker for the synthesis of HA hydrogels;[15,51,57,58] however, unlike HA–HA hydrogels which are bioactive, biocompatible, and biodegradable, HA–PEG hydrogels have limited tunability. Commercial PEG crosslinkers are typically limited to telechelic, linear, 2-, 4-, and 8-arm structures, limiting the number of reactive sites per polymer chain and requiring high amounts of crosslinker. Our data show that HA crosslinkers allow the complete tunability of gelation time of newly synthesized IEDDA hydrogels from 4.4 ± 0.4 to 46.2 ± 1.8 min whereas HA–PEG gels form only in tens of minutes at ultralow polymer content (Figure 2g). Moreover, by optimizing both the degree of substitution and the molar mass of the HA crosslinker, we can use substantially less crosslinker for a given mpT/N ratio. While the most commonly used crosslinking strategies would not be suitable for HA–HA hydrogel synthesis (i.e., limited stability of the modified polymers under physiological conditions or unavoidable degradation),[12,59,60] the IEDDA system opens up new opportunities.

The gelation properties of IEDDA HA hydrogels were further evaluated by pipettability as a function of time, HA–norbornene concentration and HA crosslinker molar mass, at the optimized mpT/N ratio of 0.25. The molar mass of the HA–methylphenyltetrazine crosslinker had the greatest impact on gelation time (Figure 2h). Interestingly, hydrogels could be pipetted beyond the theoretical gelation point measured by dynamic shear rheometry. For example, a 0.75% HA–norbornene, 240/240 (mpT/N = 0.25) IEDDA hydrogel had a theoretical gelation time of ≈4.5 min yet a pipettability time of 7.5 min, which reflects the useable time frame. This is the first report of a low polymer content (0.5–0.75%, w/v), chemically crosslinked HA-based hydrogel with tunable gelation time below 10 min under physiological conditions. Combining tunable gelation time with ultralow HA content results in hydrogels that are soft and mimic the HA content of some biological tissues, such as articular cartilage.[61]

2.6. IEDDA HA–HA Hydrogels Are Biodegradable

The biodegradability of IEDDA HA hydrogels was investigated as a function of the hyaluronidase concentration,
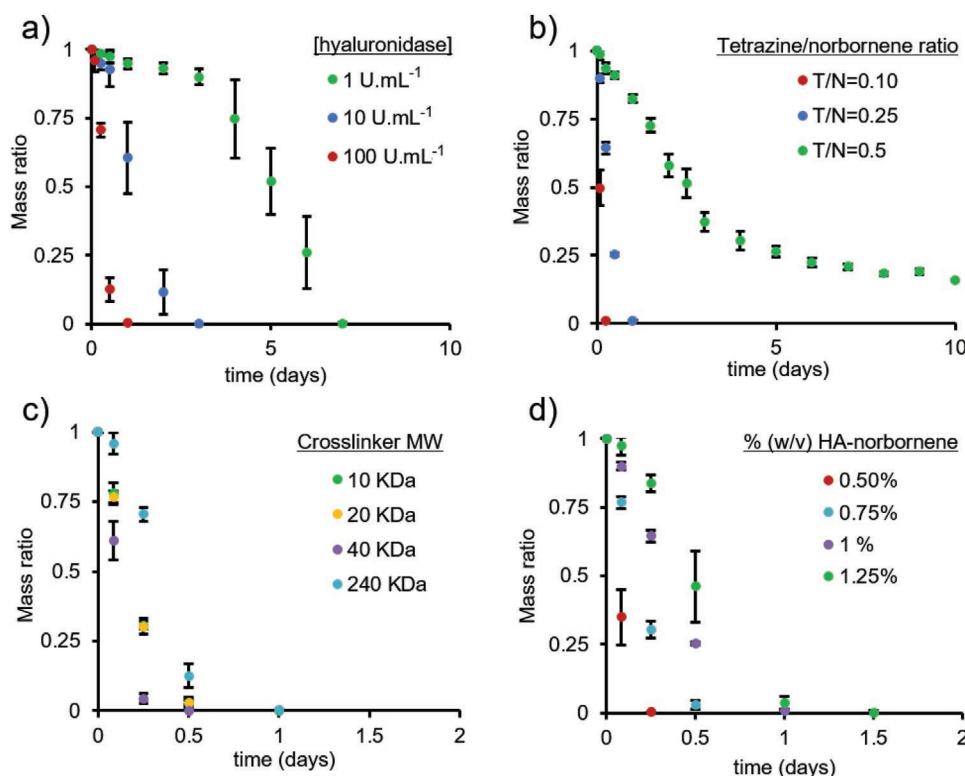
Figure 3. Biodegradability of inverse electron-demand Diels–Alder (IEDDA) HA–HA hydrogels as a function of: a) hyaluronidase concentration (1 vs 10 vs 100 U mL^{-1}), b) tetrazine to norbornene (mpT/N) molar ratio (0.1 vs 25 vs 0.5), c) molar mass of the HA–methylphenyltetrazine crosslinker (10 vs 20 vs 40 vs 240 kDa), and d) the % (w/v) HA–norbornene (0.5 vs 0.75 vs 1 vs 1.25 % (w/v)). HA–norbornene 240 kDa was used in all of the formulations. (a–c) All formulated with 0.75% (w/v) HA–norbornene, and tested with 100 U mL^{-1} hyaluronidase. The results are presented as means ± SD ($n = 3$).

methylphenyltetrazine to norbornene ratio, HA crosslinker molar mass, and polymer content (**Figure 3**). Using hyaluronidase in typical concentrations for in vitro biodegradability evaluation (1 to 100 U mL^{-1}),[51,62] our data show that optimal IEDDA HA–HA hydrogels (0.5–0.75% (w/v); mpT/N = 0.25) were fully degraded enzymatically within hours to days (Figure 3a). Interestingly, the hydrogel synthesized with an mpT/N ratio of 0.5 was not fully degraded within the 10 d assay (Figure 3b), most likely because hyaluronidase could not access and bind HA for enzymatic cleavage at this higher crosslink density. The limited degradability of both methacrylate-based or oxime-crosslinked HA hydrogels at higher polymer content and crosslink density was previously reported,[63–65] further supporting the need for low polymer content gels and optimized ratios of reactive functional groups. Using the optimal mpT/N ratio of 0.25, our data show that varying the HA crosslinker molar mass or the HA–norbornene concentration had only minor effects on the biodegradation rate of IEDDA hydrogels: all formulations tested degraded in less than 1.5 d with 100 U mL^{-1} hyaluronidase (Figure 3c,d).

2.7. IEDDA HA–HA Hydrogels Are Cytocompatible and Useful for 3D Cell Culture

The 0.5% HA–norbornene, 240/240 (mpT/N = 0.25) IEDDA hydrogel was identified as the best candidate in which to

evaluate cell survival because it had the lowest polymer content among the compositions studied and a gelation time less than 10 min. We tested the cytocompatiblity of this optimal formulation with primary cells enriched for cone-like photoreceptors dissociated from neural retina leucine zipper gene null (Nrl$^{(-/-)}$) mice.[37,66] Evaluating the stiffness of cell-encapsulating hydrogels over time, we confirmed that cell encapsulation and medium change do not alter the mechanical properties of IEDDA HA-HA hydrogels (Figure S6, Supporting Information). Nrl$^{(-/-)}$ photoreceptors that are harvested postnatally are postmitotic, and, like other primary photoreceptors cultured in vitro,[67] they die slowly over the course of a week. Using IEDDA HA–HA hydrogels, Nrl$^{(-/-)}$ photoreceptor cells were successfully encapsulated (**Figure 4**a) and showed similar viability to 2D controls over time (Figure 4b). Further experiments showed that RPE cells cultured in 3D are also viable in IEDDA HA–HA hydrogels, over at least one week (Figure S7, Supporting Information). Thus, the IEDDA norbornene–methylphenyltetrazine HA-crosslinked gels allowed viable retinal cell encapsulation, confirming the importance of fully bioorthogonal crosslinking strategies for cell encapsulation.

To deepen our understanding of hydrogel composition on retinal cell survival, various IEDDA HA–HA hydrogel formulations were further tested (Figure S8, Supporting Information). These data show that increasing the HA–norbornene concentration from 0.5% to 1% (w/v) led to a sixfold decrease in Nrl$^{(-/-)}$ photoreceptor cell survival (from 74% down to 13%)
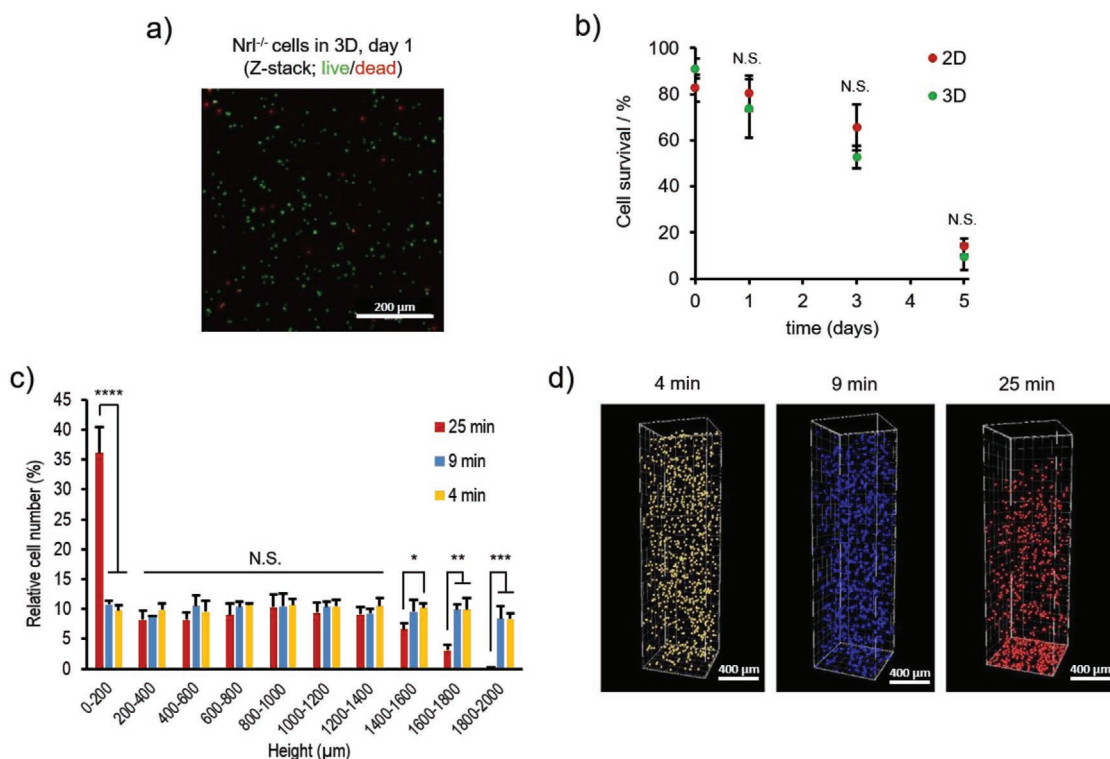
Figure 4. Optimal IEDDA HA–HA hydrogels are cytocompatible and allow homogeneous distribution of encapsulated cells. a) Representative Z-stack image of encapsulated $Nrl^{(-/-)}$ photoreceptor cells on day 1, showing high cell viability. b) Evaluation of $Nrl^{(-/-)}$ photoreceptor cell survival on 2D (glass) versus 3D (0.5% HA/HA 240/240 hydrogel, mpT/N = 0.25) culture conditions, using confocal microscopy and live/dead staining ($n = 3$; mean ± SD). c) Cell distribution of αRPE19 cells in IEDDA HA–HA hydrogels, 240/240 kDa, as a function of gelation time (4 vs 9 vs 25 min) ($n = 3$; mean ± SD). d) Representative, postgelation cell distribution of αRPE19 cells as a function of gelation time (4 vs 9 vs 25 min): cells are well-distributed with gelation times of 4 and 9 min, but not 25 min where cells accumulate at the bottom. Statistical significance was determined using one-way ANOVA with Student's t-tests in (b) and with Tukey's posthoc test in (c): N.S. = not significant, $*p < .05$, $**p < .01$, $***p < .001$, $****p < .0001$.

after 24 h, likely due to the increased crosslink density and consequent increased stiffness (400 vs 2000 Pa). The large error bars observed at 0.75% (w/v) HA–norbornene reflect the high variability of cell responses when transitioning from adequate to high mechanical constraint. This study demonstrates the role of mechanical properties on cell fate and the specific necessity of ultrasoft (≤500 Pa) hydrogels for 3D postmitotic photoreceptor cell culture.

We investigated cell distribution in our newly synthesized IEDDA HA–HA hydrogels as a function of gelation time using the tan(δ) method. Cell distribution was evaluated after 24 h and is represented as relative number of cells per 200 μm hydrogel section, over 2 mm thick gels (Figure 4c). Under optimal mixing, there should be 10% of the cells distributed evenly in each section. Hydrogels that gelled in 25 min showed considerable cell sedimentation (36% ± 4% cells in the bottom section) whereas hydrogels that gelled in 4 and 9 min had cells evenly distributed with bottom fractions having 11% ± 1% and 10% ± 1% of total cell number, respectively (Figure 4d). Cell distribution was not affected by the molar mass of HA–methylphenyltetrazine crosslinker (20 vs 240 kDa) when gelation time was kept constant (Figure S9, Supporting Information). A gelation time ≤12 min was necessary to ensure optimal cell distribution without cell sedimentation. Interestingly, in all conditions tested, either with or without cell sedimentation, the cells

within the gel fraction were homogeneously distributed, indicating proper mixing and homogeneous polymer density.

2.8. IEDDA HA–HA Hydrogels Improve Retinal Explant Multiphoton Imaging

As our new IEDDA HA–HA hydrogels were cytocompatible with retinal cells, we investigated them for retinal explant culture maintenance and laser-scanning microscopic imaging of GFP-labeled photoreceptors. Live tissue fluorescence imaging techniques are powerful tools to investigate cell behavior in intact tissues. For example, multiphoton microscopy allows whole, ex vivo, live retinal tissue imaging in vitro.[38] However, long-term (>12 h) imaging and cell tracking of fluorescent reporter signals using this technique are challenged by retinal explant viability, photodamage, and loss of fluorescence signal. Although it is necessary to immobilize retinal explants for time-series image acquisition, embedding in standard agarose thermogels is made more difficult by the growth of the retinal explant and the physical constraints of agarose, thereby limiting the effective imaging window to ≈20 h.[38] We hypothesized that the rigidity of the 1% (w/v) agarose gel (measured at 15.5 ± 1.2 kPa) impeded retinal tissue growth and, by extension, cell movement over time. Given the lower Young's modulus (≈1.1 kPa) of

**ADVANCED
SCIENCE NEWS**

www.advancedsciencenews.com

**ADVANCED
FUNCTIONAL
MATERIALS**

www.afm-journal.de

the 0.75% (w/v) IEDDA HA–HA (24/240) hydrogels, which is similar to that of retinal tissue,[68] coupled with a usable gelation time and absence of bubbles, we tested it as a replacement for agarose for retinal explant embedding. The hydrogel was applied as a viscous solution (5 to 6 min after mixing) over flattened explants on a 100 µm cell strainer membrane, and then gelled at room temperature, thereby obviating the need for heating and cooling that is required with agarose. The time to gelation was comparable to agarose, allowing immersion in the same culture medium within 10 min after embedding. The hydrogel remained intact and optically clear for at least 72 h, which was the longest time tested. Moreover, the fluorescence signal from Ccdc-136[(GFP/GFP)]-labeled (GFP) photoreceptor cells in the explants was significantly more stable over time compared to that in agarose (**Figure 5**a,b; Figure S10, Video S1, Supporting Information), which we attribute to prolonged cell survival in the softer hydrogels. The IEDDA HA–HA hydrogels effectively adhered tissue explants to the imaging platform and further reduced tissue drift in *XYZ* directions when compared to agarose. These advantages overcome the burden of postacquisition processing and frame-by-frame alignment for cell tracking. We then tested the compatibility of IEDDA HA–HA hydrogel in maintaining transfected retinal explants by electroporating postnatal day 0, GFP-retinas with CMV-H2B-dsRed plasmid (1 µg·µL^{-1}). Imaging of explants after 48 h revealed robust H2B-dsRed nuclei located in the neuroblastic layer contrasted with earlier born GFP photoreceptor cells located in the developing outer nuclear layer (Figure S11, Supporting Information). We then tested whether the application of lentivirus over IEDDA HA–HA hydrogel results in efficient infection of embedded retinal explants. A lentivirus encoding CMV-iCre was applied over IEDDA HA–HA hydrogel-embedded postnatal day 0 ROSA$^{mT/mG}$ reporter mice.[69] ROSA$^{mT/mG}$ mice express constitutive, membrane-targeted tdTomato that switches to a membrane-bound GFP following Cre-recombinase-mediated excision of the tdTomato sequence. Live imaging of infected retinal explants revealed robust lentiviral infection through the IEDDA HA–HA hydrogel (Figure S12, Supporting Information). Following culture and imaging, IEDDA HA–HA-embedded explants could be easily recovered by gentle pipetting in PBS and processed for histology (data not shown).

3. Conclusions

By tuning composition and molar mass, minimally-to-nonswelling and stable HA–HA hydrogels were formed at ultralow polymer content (<1% (w/v)) with controlled gelation times as short as 4 min. IEDDA HA gels were transparent and cytocompatible, enabling 3D culture and prolonged explant multiphoton imaging. These well-defined, click-crosslinked hydrogels lay the foundation for future in vitro and in vivo studies.

4. Experimental Section

Materials: Sodium hyaluronate with various molecular weights (10, 20, 40, and 240 kDa) was purchased from Lifecore
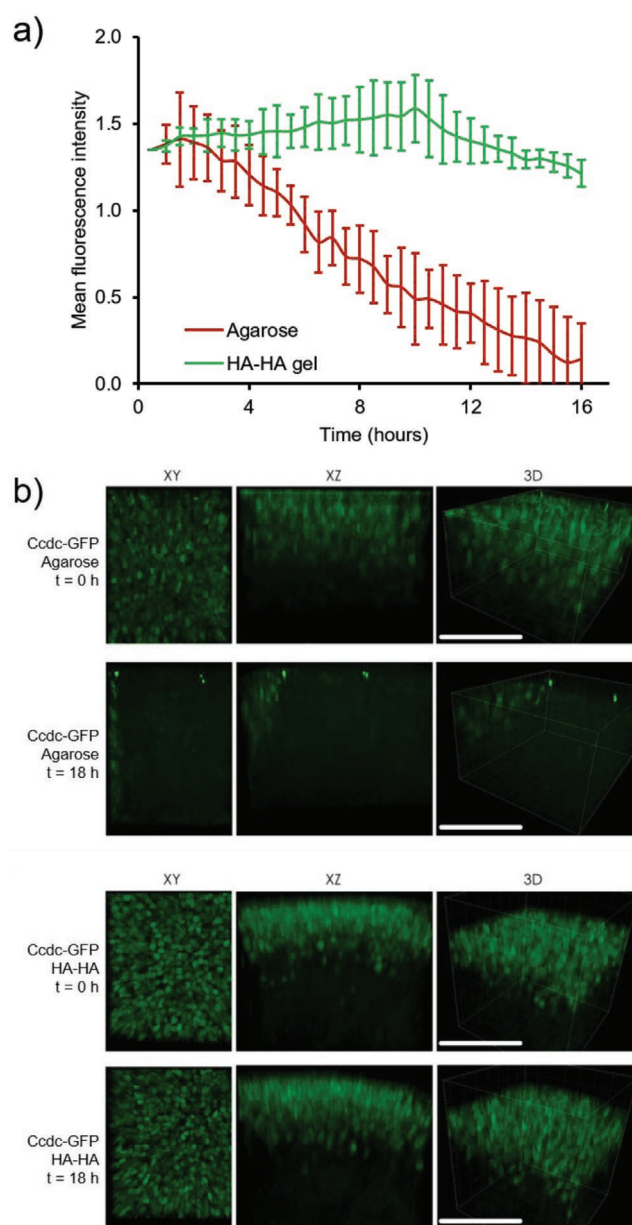

Figure 5. Inverse electron-demand Diels–Alder (IEDDA) HA–HA hydrogels improve and prolong multiphoton imaging of retinal explants. a) Change in the mean fluorescence intensity of GFP-labeled photoreceptors (*n* = 3 explants per group; mean ± SD) as a function of time and as detected by multiphoton microscopy, for retinal explants immobilized in agarose versus HA–HA hydrogels. b) Representative multiphoton images of GFP-labeled retinal explants in agarose (top) versus HA–HA gel (bottom), at 0 and 18 h, showing prolonged fluorescence in IEDDA hydrogels. *XY* = image from top, *XZ* = image from side, 3D = 3D image; scale bar = 100 µm.

Biomedical (Chaska, MN, USA). 4-(4,6-dimethoxy-1,3,5-triazin-2-yl)-4-methylmorpholinium chloride (DMT-MM) and 5-norbornene-2-methylamine (mixture of isomers) were purchased from TCI Chemicals (Portland, OR, USA). Methylphenyltetrazine-amine, HCl salt was purchased from Click Chemistry Tools (Scottsdale, AZ, USA). Hyaluronidase (998 U mL^{-1}) was purchased from Sigma-Aldrich. Dulbecco's phosphate buffered saline (without Ca & Mg) was purchased from Wisent, Inc.

**ADVANCED
SCIENCE NEWS**

www.advancedsciencenews.com

**ADVANCED
FUNCTIONAL
MATERIALS**

www.afm-journal.de

Methods: Glycosaminoglycan Modification: Synthesis of HA–Norbornene: 240 kDa HA (500 mg) was dissolved in MES buffer pH 5.5 (50 mL). DMT-MM (1.029 g; 3 eq) was added to the HA solution and allowed to react for 30 min, under stirring and at room temperature. 5-Norbornene-2-methylamine (229.3 µL; 1.5 eq) was added to the activated HA solution and allowed to react for 15 h (overnight), under stirring and at room temperature. The solution was filter-sterilized and dialyzed against 1× PBS buffer (pH 7.4) for 1 day, then deionized water for 2 d. The solution was lyophilized (MWCO 12–14 kDa, Spectrum Labs) and stored at 4 °C. The degree of substitution was determined by ^{1}H NMR (500 MHz, D_2O, δ).

Synthesis of HA–Methylphenyltetrazine: HA–methylphenyltetrazine of various MW (10, 20, 40, and 240 kDa) was synthesized, as follows: HA (200 mg) was dissolved in MES buffer pH 5.5 (20 mL). DMT-MM (137.2 mg; 1 eq) was added to the HA solution and allowed to react for 30 min, under stirring and at room temperature. Methylphenyltetrazine-amine, HCl salt (49.9 mg; 0.5 eq) was added to the activated HA solution and allowed to react for 3 d, under stirring and at room temperature. The solution was filter-sterilized and dialyzed (MWCO 2 or 12–14 kDa, Spectrum Labs) against 1× PBS buffer (pH 7.4) for 1 day, then DI water for 2 d. The solution was lyophilized and stored at 4 °C. The degree of substitution was determined by ^{1}H NMR (500 MHz, D_2O, δ).

Synthesis of PEG–Methylphenyltetrazine: Methylphenyltetrazine acid (0.29 g, 0.92 mmol) was dissolved in 10 mL of dichloromethane and activated with *N,N′*-diisopropylcarbodiimide (0.16 g, 1.31 mmol) for 1 h under nitrogen at 0 °C. 4-Arm poly(ethylene glycol) amine, HCl salt (1 g, 5 kDa) was stirred into the solution and *N,N*-diisopropylethylamine (0.25 g, 1.92 mmol) was added. After 72 h the solution was concentrated under vacuum. The crude was mixed with 20 mL of DMF and distilled water 1:1 and was dialyzed in 2 kDa molecular weight cut off membrane against 0.1 M sodium chloride followed by distilled water. The purified PEG–tetrazine was lyophilized and stored at −20 °C. The modification was determined by ^{1}H NMR (400 MHz, $CDCl_3$, δ 2.03, 3.08, 6.51, 7.52, and 8.35 ppm).

Kinetics Study of Norbornene and Methylphenyltetrazine Substitution: Norbornene and methylphenyltetrazine substitution on HA 240 kDa was investigated as a function of time using the aforementioned protocols, with 1 eq of DMT-MM and 0.5 eq of either 5-Norbornene-2-methylamine or methylphenyltetrazine-amine, HCl salt. Aliquots of substituted HA solution were taken at different time intervals, and dialyzed (MWCO 12–14 kDa, Spectrum Labs) against 1× PBS buffer (pH 7.4) for 1 d, then D.I water for 2 d, prior to lyophilization. The degree of substitution was determined by ^{1}H NMR (500 MHz, D_2O, δ).

HA–HA Hydrogel Synthesis: A typical synthesis of HA hydrogel was, as follows: in a 2 mL Eppendorf tube, HA–norbornene (7.5 mg) were dissolved in PBS (500 µL), at 37 °C for 1–2 h, prior to 10 s speedmixing (SpeedMixer DAC 150 FV2; FlackTek Inc., Landrum, USA) and 30 s microcentrifugation at max speed (14 000 rpm). A similar procedure was used to dissolve HA–methylphenyltetrazine (1.39 mg) in PBS (500 µL). In a 2 mL Eppendorf tube, HA–norbornene and HA–methylphenyltetrazine solutions were mixed together in a 1:1 volume ratio, and the prehydrogel solution was used prior to gelation.

Swelling/Stability Tests: Prehydrogel solutions were prepared as described above. Three aliquots 100 µL of prehydrogel solution was rapidly transferred in preweighed, 2 mL Eppendorf tubes, and left at 37 °C overnight for complete gelation. The gel-containing tubes were weighed, and 900 µL of warm PBS (37 °C) was added to each. At specific time points (0, 2, 6, 24, 48 h; then 4, 7, 10, 14, 21, and 28 d), the supernatant was removed, the gel surface carefully dried with Kimwipes, and the tube weighed. The swelling was determined as the ratio of a hydrogel mass at a given time point divided by its initial mass.

Biodegradation Studies: Swollen gels from swelling/stability studies were further used for the biodegradability study. Hyaluronidase (HAase) was diluted down to 1, 10, or 100 U mL^{-1} in PBS and kept at 4 °C. The enzyme solution was rapidly warmed up to 37 °C prior to use, and stored at 4 °C between time points. The gel-containing tubes were weighed, and 900 µL of warm hyaluronidase solution was added. At specific time points (0, 2, 6, 24, 48 h; then 4, 7, 10 d), the supernatant was removed,

the gel surface carefully dried with Kimwipes, and the tube weighed. The mass ratio, determined as the ratio of a hydrogel mass at a given time point over its initial mass, was used as a proxy for biodegradation.

Gelation Time Measurements: Gelation time by Rheometry: Prehydrogel solutions were prepared as described above. Gelation data were collected using a TA Instruments AR1000 rheometer (New Castle, DE, USA), equipped with a 1° acrylic cone (40 mm) and a Peltier plate for temperature control. A solvent trap was used to minimize evaporation during the measurements. Gels were first equilibrated for 30 s at 23 °C. Then the loss tangent, tan(δ), defined as the ratio of the shear loss modulus (G'') to the shear storage modulus (G'), was measured as a function of time. The measurements were performed at two different angular frequencies in the terminal zone (0.1 and 0.2 Hz), using 1% strain, which was confirmed to be in the linear viscoelastic region of the material studied.

Gelation time by Pipettability: Prehydrogel solutions were prepared as described above. In 2 mL Eppendorf tubes, 200 µL prehydrogel aliquots were tested for pipettability every 2.5 min, using a 200 µL micropipette equipped with a standard tip. The gelation time was considered as the time when no gel can be taken up by the pipette, with time zero corresponding to HA–norbornene and HA–methylphenyltetrazine mixing.

Young's Modulus Measurement: Prehydrogel solutions were prepared as described above. Four aliquots of 100 µL of prehydrogel solution were rapidly transferred in a 16-well chamber slide (Nunc Lab-Tek Chamber Slide; Thermo Fisher Scientific), and left at 37 °C overnight for complete gelation. The chamber slide bottom was detached and the gels were gently taken out of the wells for measurements. Young's modulus was measured using a mechanical tester (Mach-1 Micromechanical System, Biomomentum). The gel thickness was first determined using the find contact mode, with a stage velocity of 0.005 mm s^{-1} and a contact criteria of 0.075 g. The Young's modulus was then measured using the stress relaxation mode: the gel was first compressed by 10 % of its initial thickness, prior to 5 × 30 s relaxation measurements, with a ramp amplitude corresponding to 2 % of its initial thickness, and ramp velocity corresponding to 2 % of the thickness. The Young's modulus was calculated from the average slope of Force (N m^{-1}) versus time (s), the gel thickness (m), and the surface area (m^2).

Transparency and Refractive Index: Prehydrogel solutions were prepared as described above. A 100 µL prehydrogel was rapidly transferred in a 96-well plate and gelled at either room temperature or 37 °C. The absorbance of the HA hydrogel was measured (TECAN plate-reader, Infinite M200 Pro; 300–800 nm) at different time intervals (0, 1, 3, 5, 7, 24 h), from which transmittance was calculated. Time zero corresponds to the time of HA–norbornene and HA–methylphenyltetrazine mixing. Refractive index of 0.75 % HA-only hydrogel (mpT/N = 0.25) was measured using a refractometer, both before and after gelation.

Retinal Cell Encapsulation Study: Animals: All experiments were approved by the University Health Network Research Ethics Board and adhered to the guidelines of the Canadian Council on Animal Care. Animal husbandry was performed in accordance with the Association for Research in Vision and Ophthalmology (ARVO) Statement for the Use of Animals in Ophthalmic and Vision Research. Animals were maintained under standard laboratory conditions and all procedures were performed in conformity with the University Health Network Animal Care Committee (protocol 3499.14.2). For Ccdc-136$^{(GFP/GFP)}$ cone photoreceptor reporter mice (Smiley et al., 2016) were genotyped using genomic ear clip DNA and incubation in 200 µL alkaline lysis buffer (25 × 10^{-3} M NaOH, 0.2 × 10^{-3} M EDTA pH 8.0) for 1 h at 95 °C. Samples were neutralized with 200 µL neutralization buffer (40 × 10^{-3} M Tris-HCl) and genotyped using primers as previously described.[66,70]

Nrl$^{(-/-)}$ Photoreceptor Cell Preparation: To prepare Nrl$^{(-/-)}$ cells for in vitro experiments, retinas from Nrl$^{(-/-)}$ mice at postnatal day 3–5 were harvested in CO_2 independent media (Fisher Scientific) and dissociated with papain (Worthington Biochemical, UK) according to the manufacturer's directions. Cells were washed in Ca^{2+}/Mg^{2+} free PBS and counted using 0.4% Trypan blue (Thermo Fisher) as a viability counter stain before being resuspended in media.

αRPE-19 Cell Preparation: αRPE-19 cells were cultured in DMEM/F-12 with 10% fetal bovine serum. The cells were fed every other day, and passaged every 4–5 days. Cells were used between P4 and P10.

Cell Survival Studies: HA–norbornene and HA–methylphenyltetrazine solutions were prepared following a similar protocol as above, under sterile conditions, using the appropriate cell medium to dissolve the gel components, and adjusting the HA–methylphenyltetrazine concentration to account for a small volume of retinal cells to mix in a typical HA–norbornene/HA–methylphenyltetrazine/cell volume ratio was 1/0.5/0.5. 1×10^6 cells in 0.5 mL were first mixed with 1 mL of HA–norbornene. Then, 0.5 mL of HA–methylphenyltetrazine was mixed with the HA–norbornene/cell solution, and the prehydrogel solution obtained was rapidly plated in a 16-well chamber slide (Nunc Lab-Tek Chamber Slide; Thermo Fisher Scientific). The cell-containing hydrogels (100 μL) were incubated (37 °C, 5% CO_2, 95% humidity) for 2 h before adding 150 μL of cell medium on top, prior to prolonged incubation periods. In 3D conditions (HA hydrogel), cells were cultured at a density of 5×10^4 cells per well, and fed every other day. A 2D control was performed, culturing cells on glass at a density of 2×10^4 cells per well, in 250 μL cell medium, with feeding every other day. Cell viability was assessed via live/dead staining and confocal microscopy (Olympus FV1000), using Calcein AM (live cells, Sigma-Aldrich), ethidium homodimer (dead cells, Sigma-Aldrich), and Hoechst (all cell control, Invitrogen), as per the manufacturer's instructions. Average viability was obtained from three biological replicates, and measured every other day over 5–7 days.

Cell Distribution Evaluation: αRPE-19 cells were encapsulated and stained in HA-only hydrogels as described above. Cell distribution as a function of gelation time was evaluated from three biological replicates by confocal microscopy (Olympus FV1000), at day 1. Using the rheometry data as references, three gelation times (4, 9, and 25 min) were tested, corresponding to three hydrogel compositions (0.75%, 0.5%, and 0.25% HA–norbornene, respectively; all with HA–methylphenyltetrazine 240 kDa at a mpT/N ratio of 0.25). Cell number per 100 μm section was evaluated, with cells at the bottom counted separately. Cell distribution was calculated as cumulative cell number per volume of gel, with both cell number and volume normalized for comparison and averaged.

Multiphoton and Confocal Imaging of Postnatal Retinal Explants: Postnatal Retinal Explant Isolation: All live imaging experiments were approved by the University Health Network Research Ethics Board (protocol 3499.10) under the guidelines of the Canadian Council on Animal Care. Husbandry was in accordance with the ARVO Statement for the Use of Animals in Ophthalmic and Vision Research. Postnatal day 0 Ccdc-136$^{(GFP/GFP)}$ mice were sacrificed by decapitation and eyes were enucleated in a sterile microzone cabinet as previously described.[38] Briefly, intact retinas were carefully dissected in a dissection dish containing prewarmed CO_2-independent media (Thermo Fisher Scientific, 18045088). Four cuts were made to generate a Maltese cross flat mount preparation, which was then washed in Hank's Balanced Salt Solution without calcium or magnesium. For transfection experiments, in vitro electroporation of CMV-NLS-mCherry (Addgene plasmid #108881 – Rob Parton Lab)[71] was performed as previously described.[38]

Embedding of Retinal Explants for Live Imaging: For agarose embedding, 0.01 g of low-melting temperature agarose (Gibco BRC) was dissolved in 1 mL CO_2-independent medium and maintained at 42 °C. Isolated retinas were placed ganglion cell down on falcon-brand cell strainers adapted to a premade live imaging chamber as described previously.[38] Excess media was removed using a 200 μL tip followed by cotton stabs to dry the membrane pores. Approximately 20 μL of the agarose solution was pipetted onto the retinal explants, allowing the gel to intercalate with the membrane pores, followed by transfer of the imaging chamber to 4 °C for 5 min. Live imaging medium (CO_2-independent media containing 1 × Glutamax and 1 × B27 supplement) was added over top of the agarose embedded explant. For hydrogel embedding, ≈20 μL of cold IEDDA HA–HA hydrogel (4 °C) was s added over top of explants, followed by 15 min of gelation time before covering with live imaging medium.

Multiphoton Imaging and Analysis: Live imaging chambers were filled with 80 mL of live imaging medium and transferred to a dual beam Leica TCS SP8 multiphoton microscope equipped with a 1300 nm Chameleon Discovery laser (Coherent). An HC IRAPO L 25×/1.00 W, 1.95 mm working-distance objective lens equipped with a motorized correction collar was lowered into the imaging arena. The objective was positioned over the midpoint of the retina, between the optic disk and the margin under epifluorescence. Before data acquisition, explant media was equilibrated for 3 h to a temperature of 35 °C using a Leica MATS TPX heated stage insert with a media temperature probe. For imaging of Ccdc-136$^{(GFP/GFP)}$ cones, the laser was tuned to 960 nm and power output maintained at 45 mW for all samples to control for photobleaching. Emitted visible light was captured using an internal HyD SP GaAsP hybrid detector gated to a range of 500–525 nm emission. Z-stack images were acquired at 30 min intervals for up to 18 h. Acquisition settings were 2.5× zoom, 2× accumulation, 2× averaging, 0.70 μm z-resolution, and 960 × 960 xy resolution. Time-series image files were concatenated using the Leica LAS X software and transferred to Imaris 9.1 for postacquisition analysis. The mean fluorescence intensity was measured in Imaris 9.1, and data were normalized such that both conditions had the same intensity values at the onset of imaging.

Statistical Analysis: All in vitro data are presented as mean ± standard deviation. Statistical analyses were performed using GraphPad, evaluating statistical significance by Student's *t*-test or one-way ANOVA with Tukey's posthoc test, when applicable.

Supporting Information

Supporting Information is available from the Wiley Online Library or from the author.

Acknowledgements

Conflict of Interest

The authors declare no conflict of interest.

Keywords

[1] J. Y. Lee, A. P. Spicer, *Curr. Opin. Cell Biol.* **2000**, *12*, 581.
[2] S. P. Evanko, M. I. Tammi, R. H. Tammi, T. N. Wight, *Adv. Drug Delivery Rev.* **2007**, *59*, 1351.
[3] D. G. Jackson, *Immunol. Rev.* **2009**, *230*, 216.
[4] K. S. Girish, K. Kemparaju, *Life Sci.* **2007**, *80*, 1921.
[5] N. Itano, *J. Biochem.* **2008**, *144*, 131.
[6] E. Puré, R. K. Assoian, *Cell. Signalling* **2009**, *21*, 651.
[7] R. Y. Tam, L. J. Smith, M. S. Shoichet, *Acc. Chem. Res.* **2017**, *50*, 703.

**ADVANCED
SCIENCE NEWS**
www.advancedsciencenews.com

**ADVANCED
FUNCTIONAL
MATERIALS**
www.afm-journal.de

[8] S. R. Caliari, J. A. Burdick, *Nat. Methods* **2016**, *13*, 405.

[9] S. Kirchhof, F. P. Brandl, N. Hammer, A. M. Goepferich, *J. Mater. Chem. B* **2013**, *1*, 4855.

[10] J. Kalia, R. T. Raines, *Angew. Chem., Int. Ed.* **2008**, *47*, 7523.

[11] R. C. Boutelle, B. H. Northrop, *J. Org. Chem.* **2011**, *76*, 7994.

[12] X. Z. Shu, Y. Liu, Y. Luo, M. C. Roberts, G. D. Prestwich, *Biomacromolecules* **2002**, *3*, 1304.

[13] L. Maleki, U. Edlund, A.-C. Albertsson, *Biomacromolecules* **2015**, *16*, 667.

[14] C. B. Rodell, N. N. Dusaj, C. B. Highley, J. A. Burdick, *Adv. Mater.* **2016**, *28*, 8419.

[15] L. J. Smith, S. M. Taimoory, R. Y. Tam, A. E. G. Baker, N. Binth Mohammad, J. F. Trant, M. S. Shoichet, *Biomacromolecules* **2018**, *19*, 926.

[16] C. M. Madl, S. C. Heilshorn, *Adv. Funct. Mater.* **2018**, *28*, 1706046.

[17] B. L. Oliveira, Z. Guo, G. J. L. Bernardes, *Chem. Soc. Rev.* **2017**, *46*, 4895.

[18] S. T. Koshy, R. M. Desai, P. Joly, J. Li, R. K. Bagrodia, S. A. Lewin, N. S. Joshi, D. J. Mooney, *Adv. Healthcare Mater.* **2016**, *5*, 541.

[19] S. Hong, J. Carlson, H. Lee, R. Weissleder, *Adv. Healthcare Mater.* **2016**, *5*, 421.

[20] R. M. Desai, S. T. Koshy, S. A. Hilderbrand, D. J. Mooney, N. S. Joshi, *Biomaterials* **2015**, *50*, 30.

[21] A. Lueckgen, D. S. Garske, A. Ellinghaus, R. M. Desai, A. G. Stafford, D. J. Mooney, G. N. Duda, A. Cipitria, *Biomaterials* **2018**, *181*, 189.

[22] D. L. Alge, M. A. Azagarsamy, D. F. Donohue, K. S. Anseth, *Biomacromolecules* **2013**, *14*, 949.

[23] H. Zhang, K. T. Dicker, X. Xu, X. Jia, J. M. Fox, *ACS Macro Lett.* **2014**, *3*, 727.

[24] A. Famili, K. Rajagopal, *Mol. Pharmaceutics* **2017**, *14*, 1961.

[25] M. R. Karver, R. Weissleder, S. A. Hilderbrand, *Bioconjugate Chem.* **2011**, *22*, 2263.

[26] M. M. Le Goff, P. N. Bishop, *Eye* **2008**, *22*, 1214.

[27] J. G. Hollyfield, M. E. Rayborn, M. Tammi, R. Tammi, *Exp. Eye Res.* **1998**, *66*, 241.

[28] J. G. Hollyfield, *Invest. Ophthalmol. Visual Sci.* **1999**, *40*, 2767.

[29] M. Ishikawa, Y. Sawada, T. Yoshitomi, *Exp. Eye Res.* **2015**, *133*, 3.

[30] M. Inatani, H. Tanihara, *Prog. Retinal Eye Res.* **2002**, *21*, 429.

[31] B. G. Ballios, M. J. Cooke, L. Donaldson, B. L. K. Coles, C. M. Morshead, D. van der Kooy, M. S. Shoichet, *Stem Cell Rep.* **2015**, *4*, 1031.

[32] N. Mitrousis, R. Y. Tam, A. E. G. Baker, D. van der Kooy, M. S. Shoichet, *Adv. Funct. Mater.* **2016**, *26*, 1975.

[33] M. A. J. Mazumder, S. D. Fitzpatrick, B. Muirhead, H. Sheardown, *J. Biomed. Mater. Res., Part A* **2012**, *100A*, 1877.

[34] Y. Liu, R. Wang, T. I. Zarembinski, N. Doty, C. Jiang, C. Regatieri, X. Zhang, M. J. Young, *Tissue Eng., Part A* **2013**, *19*, 135.

[35] N. C. Hunt, D. Hallam, A. Karimi, C. B. Mellough, J. Chen, D. H. W. Steel, M. Lako, *Acta Biomater.* **2017**, *49*, 329.

[36] O. Strauss, *Physiol. Rev.* **2005**, *85*, 845.

[37] L. L. Daniele, C. Lillo, A. L. Lyubarsky, S. S. Nikonov, N. Philp, A. J. Mears, A. Swaroop, D. S. Williams, E. N. J. Pugh, *Invest. Opthalmol. Visual Sci.* **2005**, *46*, 2156.

[38] P. E. B. Nickerson, K. M. Ronellenfitch, N. F. Csuzdi, J. D. Boyd, P. L. Howard, K. R. Delaney, R. L. Chow, *BMC Dev. Biol.* **2013**, *13*, 24.

[39] A.-C. Knall, C. Slugovc, *Chem. Soc. Rev.* **2013**, *42*, 5131.

[40] S. Eising, A. H. J. Engwerda, X. Riedijk, F. M. Bickelhaupt, K. M. Bonger, *Bioconjugate Chem.* **2018**, *29*, 3054.

[41] *Multiphase Flow Dynamics 1* (Ed: N. I. Kolev), Springer, Berlin **2007**, pp. 185–214.

[42] J. Yang, Y. Liang, J. Seckute, K. N. Houk, N. K. Devaraj, *Chem. - Eur. J.* **2014**, *20*, 3365.

[43] H. Kamata, Y. Akagi, Y. Kayasuga-Kariya, U. Chung, T. Sakai, *Science* **2014**, *343*, 873.

[44] T. M. O'Shea, A. A. Aimetti, E. Kim, V. Yesilyurt, R. Langer, *Adv. Mater.* **2015**, *27*, 65.

[45] H. Chen, F. Yang, R. Hu, M. Zhang, B. Ren, X. Gong, J. Ma, B. Jiang, Q. Chen, J. Zheng, *J. Mater. Chem. B* **2016**, *4*, 5814.

[46] S.-H. Lee, C.-W. Park, S.-G. Lee, W.-K. Kim, *Korean J. Spine* **2013**, *10*, 44.

[47] H. Kamata, K. Kushiro, M. Takai, U. Chung, T. Sakai, *Angew. Chem., Int. Ed.* **2016**, *55*, 9282.

[48] L. J. Macdougall, M. M. Pérez-Madrigal, M. C. Arno, A. P. Dove, *Biomacromolecules* **2018**, *19*, 1378.

[49] V. X. Truong, K. M. Tsang, J. S. Forsythe, *Biomacromolecules* **2017**, *18*, 757.

[50] Y.-W. Kim, J. E. Kim, Y. Jung, J.-Y. Sun, *Mater. Sci. Eng., C* **2019**, *95*, 86.

[51] A. E. G. Baker, R. Y. Tam, M. S. Shoichet, *Biomacromolecules* **2017**, *18*, 4373.

[52] K. Dušek, *Polym. Gels Networks* **1996**, *4*, 383.

[53] H. H. Winter, *Polym. Eng. Sci.* **1987**, *27*, 1698.

[54] F. Yu, F. Zhang, T. Luan, Z. Zhang, H. Zhang, *Polymer* **2014**, *55*, 295.

[55] P. J. Flory, *J. Phys. Chem.* **1942**, *46*, 132.

[56] W. H. Stockmayer, *J. Chem. Phys.* **1944**, *12*, 125.

[57] S. C. Owen, S. A. Fisher, R. Y. Tam, C. M. Nimmo, M. S. Shoichet, *Langmuir* **2013**, *29*, 7393.

[58] R. Y. Tam, S. A. Fisher, A. E. G. Baker, M. S. Shoichet, *Chem. Mater.* **2016**, *28*, 3762.

[59] H. Tan, J. P. Rubin, K. G. Marra, *Macromol. Rapid Commun.* **2011**, *32*, 905.

[60] H. Tan, H. Li, J. P. Rubin, K. G. Marra, *J. Tissue Eng. Regener. Med.* **2011**, *5*, 790.

[61] M. K. Cowman, H.-G. Lee, K. L. Schwertfeger, J. B. McCarthy, E. A. Turley, *Front. Immunol.* **2015**, *6*, 261.

[62] J. A. Burdick, C. Chung, X. Jia, M. A. Randolph, R. Langer, *Biomacromolecules* **2005**, *6*, 386.

[63] S. K. Hahn, J. K. Park, T. Tomimatsu, T. Shimoboji, *Int. J. Biol. Macromol.* **2007**, *40*, 374.

[64] J. Patterson, R. Siew, S. W. Herring, A. S. P. Lin, R. Guldberg, P. S. Stayton, *Biomaterials* **2010**, *31*, 6772.

[65] J. G. Hardy, P. Lin, C. E. Schmidt, *J. Biomater. Sci., Polym. Ed.* **2015**, *26*, 143.

[66] S. Smiley, P. E. Nickerson, L. Comanita, N. Daftarian, A. El-Sehemy, E. L. S. Tsai, S. Matan-Lithwick, K. Yan, S. Thurig, Y. Touahri, R. Dixit, T. Aavani, Y. De Repentigny, A. Baker, C. Tsilfidis, J. Biernaskie, Y. Sauve, C. Schuurmans, R. Kothary, A. J. Mears, V. A. Wallace, *Sci. Rep.* **2016**, *6*, 22867.

[67] V. Fontaine, N. Kinkl, J. Sahel, H. Dreyfus, D. Hicks, *J. Neurosci.* **1998**, *18*, 9662.

[68] D. L. Hugar, A. Ivanisevic, *Mater. Sci. Eng., C* **2013**, *33*, 1867.

[69] M. D. Muzumdar, B. Tasic, K. Miyamichi, L. Li, L. Luo, *Genesis* **2007**, *45*, 593.

[70] A. Ortin-Martinez, E. L. S. Tsai, P. E. Nickerson, M. Bergeret, Y. Lu, S. Smiley, L. Comanita, V. A. Wallace, *Stem Cells* **2017**, *35*, 932.

[71] N. Ariotti, J. Rae, N. Giles, N. Martel, E. Sierecki, Y. Gambin, T. E. Hall, R. G. Parton, *PLoS Biol.* **2018**, *16*, e2005473.